

CORONARY PLAQUE CLASSIFICATION WITH ACCUMULATIVE TRAINING OF DEEP BOLTZMANN MACHINES

KUONG TRONG NGUYEN¹, EIJI UCHINO^{2,3} AND NORIAKI SUETAKE²

¹Faculty of Information Technology
Vietnam National University of Agriculture
Gialam, Hanoi 131-046, Vietnam
ntkuong@vnua.edu.vn

²Graduate School of Science and Technology for Innovation
Yamaguchi University
1677-1 Yoshida, Yamaguchi 753-8512, Japan
{ uchino; suetake }@sci.yamaguchi-u.ac.jp

³Fuzzy Logic Systems Institute
680-41 Kawazu, Iizuka 820-0067, Japan

Received February 2018; accepted May 2018

ABSTRACT. *Using powerful classification frameworks to handle with large data sets has attracted much attention in medical applications. This study shows an application of deep Boltzmann machines (DBM's) to characterize intravascular ultrasound (IVUS) signals of coronary plaque. Our problem is to recognize coronary plaque tissues from IVUS signals. In the IVUS data sets, the data normalization is affected by near field artifacts; thus it gives rise to difficulties of the classification by DBM's. Additionally, there are significant imbalances between tissue classes. In solution, we introduce an accumulative selection of training sets which is sensitive to misclassification rates to deal with class imbalances while the IVUS data set is concerned at binary level. The results show that the proposed method performs better than integrated backscatter IVUS method (IB-IVUS) for the same task.*

Keywords: Coronary plaque, Intravascular ultrasound, Deep Boltzmann machines, Class imbalances

1. **Introduction.** Blood flow becomes restricted when coronary plaque develops inside arteries. More seriously, blood flow can be blocked if the plaque destabilizes and ruptures. In pathology research, the evaluation of atherosclerotic plaque progression and its rupture-prone risk is a crucial task in order to prevent its fatal consequences. IVUS technique allows to investigate plaque built up inside artery thanks to ultrasound. From those acquired ultrasound signals, plaque tissues are characterized by a computerized program for further consideration of medical diagnosis.

To evaluate plaque structure, it requires careful steps from data acquisition to classification [1]. Often, acquired IVUS signals are analyzed thanks to methodologies of signal processing and pattern recognition. There are various approaches to process IVUS signals from signal preprocessing to pattern extraction, and data representation such as time and fequency domain. In addition, each IVUS analysis method designates a classification model which is trained to learn the distribution of predetermined features. For example, integrated backscatter (IB-IVUS) [2] is a method which analyzes power spectrum of IVUS signals and calculates the IB values as the features for tissue classification, or, Nair et al. [3] proposed autoregressive classification model.

Machine learning has become a great concern in medical applications because it provides some powerful learning models for handling big data sets. In the field of machine learning,

deep learning [4] has attracted enthusiastic interest in recent years, which is architected by a deep network to handle with large, high-dimensional data sets. Restricted Boltzmann machine (RBM) is a good initiation for constructing multiple-layer network [4,5]. It is a probabilistic model that contains a layer of hidden binary variables connecting to a visible layer of visible variables, and the hidden layer will model the distribution of visible layer [6,7].

RBM itself can play as a self-contained framework as a classification model [8]. Originally, RBMs were developed using binary stochastic units for both input and hidden layers, and the extension to Gaussian visible inputs was also implemented [6]. The latter case employs data normalization to transform data sets into unit interval or standard normal distribution. In [9-11], we used the standalone model of RBM for the classification of IVUS tissues. However, IVUS signals are affected by near field artifacts, i.e., it results in high amplitudes surrounding transducer [12]. We observed that the data normalization of IVUS signals is significantly affected by those artifacts [9]. In addition, the class imbalances of IVUS training data sets give rise to difficulties of tissue classification.

Pursuing a deep network to learn complicated IVUS data sets better, in this study, we are interested in deep Boltzmann machines (DBM's) [13] that is constructed by stacking restricted Boltzmann machines (RBM's). We employ a quantization domain to extract binary featured patterns for DBM to avoid near field artifacts by normalization.

This paper is organized as follows. Section 2 presents our method with the description of DBM network, pattern extraction for the classification and the proposed solution to deal with class imbalances. Section 3 shows the experiments and results. Finally, Section 4 will conclude the study.

2. Methodology.

2.1. Deep Boltzmann machines. The DBM network we use in this study is shown in Figure 1 with two hidden layers h^1 and h^2 where x , y are visible and class layers. Architecturally, the DBM includes RBM with (x, h^1) and classification RBM with (h^1, h^2, y) . The first RBM transforms data into low-dimensional codes for the classification of the latter one. We call coding phase and classification phase correspondingly.

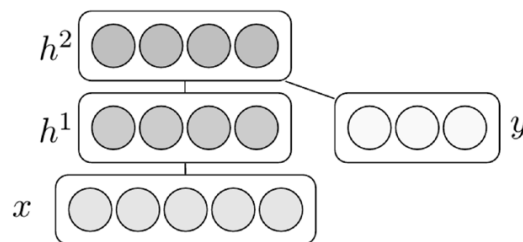


FIGURE 1. Deep Boltzmann machine network with two hidden layers

In coding phase, RBM is trained by stochastic contrastive divergence [6]. In classification phase, we use discriminative training of classification RBM. In prediction, class j of input x is defined by:

$$j = \underset{i}{\operatorname{argmax}} P(y_i | h^1, x). \quad (1)$$

The readers can refer to [8] for further detail.

2.2. Pattern extraction. Figure 2 illustrates the patch extraction where Figure 2(a) is about a stained vessel section. Its B-mode image is displayed in Figure 2(b). Plaque is drawn as in Figure 2(c) whereas plaque is drawn by lines with fibrous, fibrofatty and fatty areas denoted A, B, C, respectively. Time-series signals (A-lines) of vessel section in Figure 2(a) are longitudinally shown in Figure 2(d). We extracted patches of $M \times N$

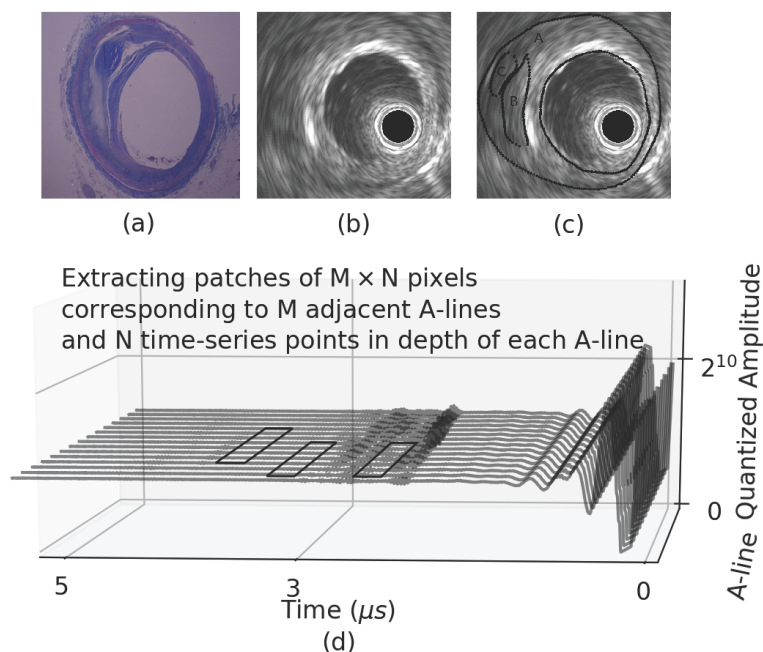


FIGURE 2. Patch extraction from time-series IVUS signals. Picture (a) shows a stained vessel image with B-mode display in (b). Three tissue components fibrous, fibrofatty and fatty are detected by experts as denoted A, B, C, respectively.

pixels as window frames in Figure 2(d) whereas A, B, C denote fibrous, fibrofatty and fatty areas in Figure 2(c), respectively. Each patch corresponds to an $M \times N$ matrix of quantized amplitudes which were integer-valued ones received from a 12-bit analog-to-digital converter (ADC) of the IVUS transducer. Then, those quantized amplitudes are represented in binary series of 12 bits the same as the IVUS transducer quantization size. In one rough interpretation, this work is understood that 12 visible units of the DBM are allocated to encode an amplitude.

2.3. Dealing with class imbalances. Our IVUS data sets concern three tissue classes: fibrous, fibrofatty and fatty. In fact, the distribution of classes is considerably different, and fibrous often outreprents the rests. Fatty accounts only around 2 percent of the data sets. To deal with the difficulty of class imbalances, in each training epoch of the classification phase of DBM, we reselect the training volume of each class. We follow the idea of the cost-sensitive training scheme in [14] to update the volume of training sets. Shortly speaking, the number of each sub-class chosen for training is accumulated so that it depends on the training cost of previous training step. Here, misclassification rate is defined as training cost. Due to class imbalances, the cost differs between classes so the training sets should be updated in proportions to the misclassification rate of each class.

Specifically, let n_{i*} be the number of samples in class i of training sets, where n_{ij} is the number of i -class samples which are classified in class j . Then, the misclassification rate of class i , say $Miss_i$, is defined by:

$$Miss_i = \sum_{j \neq i} n_{ij} / n_{i*}. \quad (2)$$

Now, we add superscript (k) to n_{ij} and $Miss_i$, those are $n_{ij}^{(k)}$, $Miss_i^{(k)}$, to define that they are calculated at the k -th training iteration. Let $n_i^{(k)}$ be the number of i -class training inputs which are chosen at step k . With the above assumption of cost sensitiveness, we

define the number of i -class training input samples at step $k + 1$ by:

$$n_i^{(k+1)} = n_i^{(k)} + \left[\alpha \times n_{i^*} \times \left(\text{Miss}_i^{(k)} - \min_j \text{Miss}_j^{(k)} \right) \right]. \quad (3)$$

Here, $[\cdot]$ is a round function. In case $n_i^{(k+1)} > n_{i^*}$, i.e., the number of i -class samples defined by Equation (3) is greater than the number of i -class samples in the training sets, oversampling is used, otherwise undersampling is used. For oversampling, we use replication. Equation (3) describes the accumulative training volume of each class. The real number α is introduced to control the updated number of training samples. Obviously, if at step k , the misclassification rate is minimized by class i , then the number of i -class samples is unchanged in the next training iteration.

3. Experiments and Results. The research data sets were provided by the Graduate School of Medicine, Yamaguchi University. Six vessel sections of human left circumflex coronary artery were involved in this study. The ultrasonic observation was carried out using a Galaxy IVUS system (Boston, USA) with a 40 MHz transducer at rotation speed of 30 revs/s, and 256 A-lines were collected in one revolution. The analog signals were sampled at the sampling rate of 210 MHz and quantized by a 12 bit ADC.

We used three coronary sectional images for training and three others for test. Table 1 shows the number of each class in data sets. Patches are extracted with five cases of size: 3×5 , 5×9 , 5×17 , 5×25 and 7×17 of pixels, and then those patches are represented in 12 bit series as binary stored by the IVUS transducer.

In settings, we set α of Equation (3) equal to 0.1, and the number of iterations equal to 200 in all the cases of classification phase.

Figure 3 shows the classification of test case for the cases of patch sizes whereas the DBM has a network size of 500-150, i.e., 500 units of the first hidden layer and 150 units of the second one. The results are also compared with the performance of IB-IVUS method for the same volumn size. The classification performances are assessed by G-mean which is the geometric average of true positive rates (TPR) of all classes. Clearly, the G-means by the proposed method are significantly improved as compared to the conventional method IB-IVUS.

TABLE 1. Number of each tissue class in data sets

	fibrous	fibrofatty	fatty
Training sets	106,002	12,582	4,585
Test sets	89,440	13,880	3,898

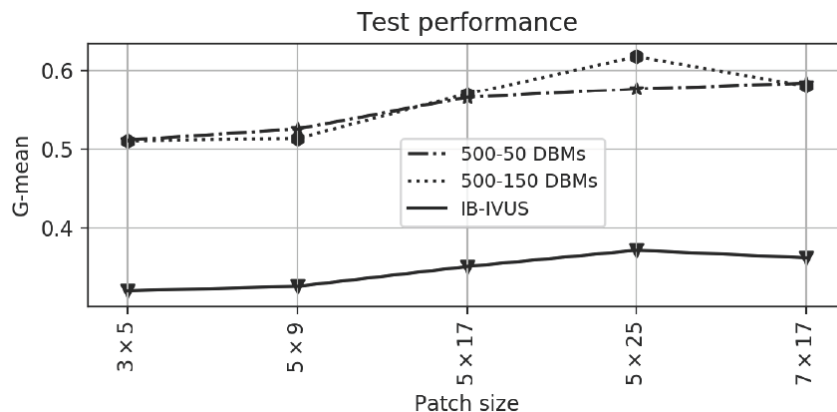


FIGURE 3. Classification of DBM in the cases of patch size

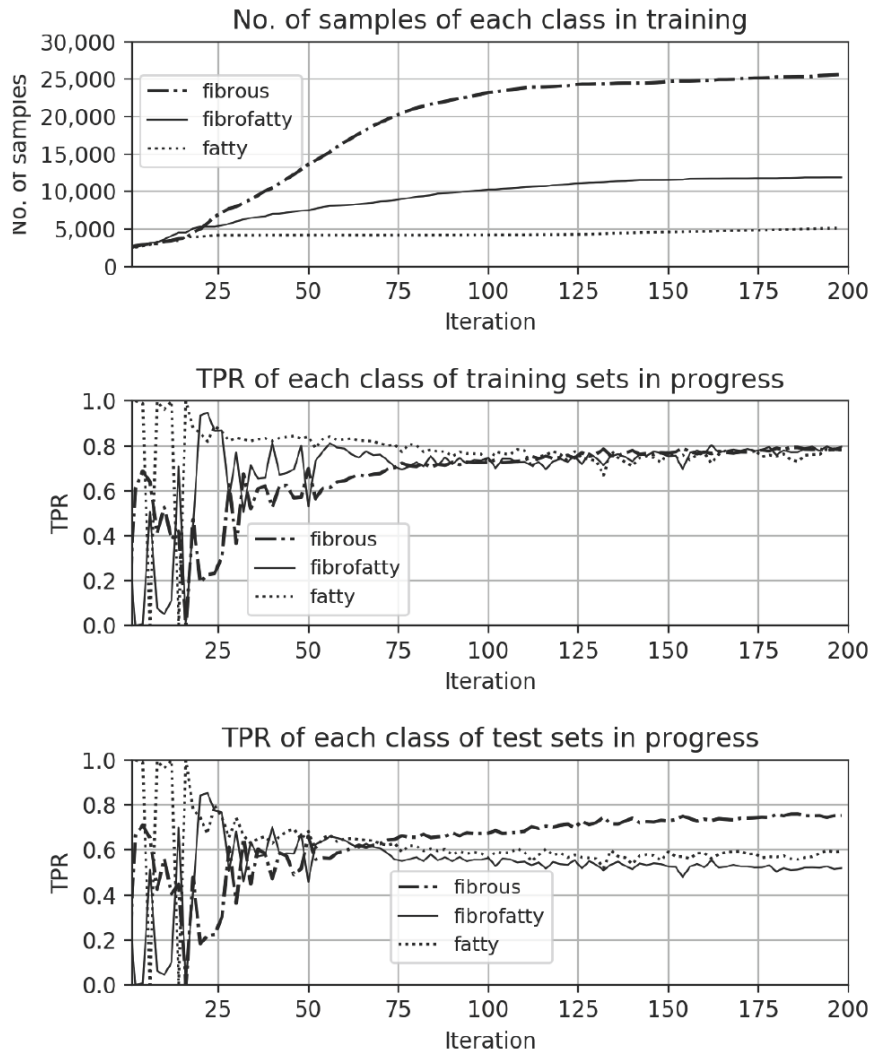


FIGURE 4. Number of samples in each class by Equation (3) and the TPR progress of each class achieved by 500-150 DBM with the patch size case of 5×25

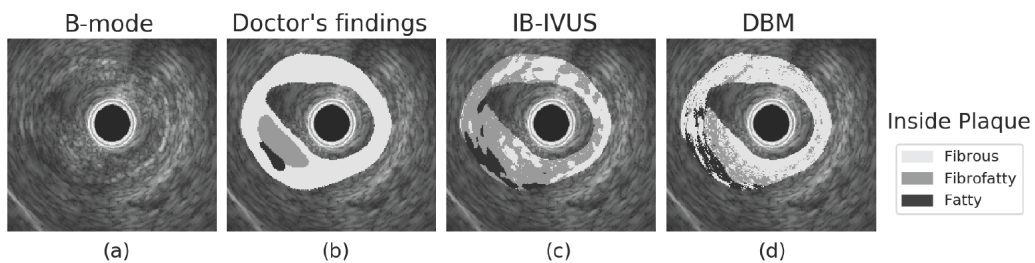


FIGURE 5. Classification performance of one test vessel section by IB-IVUS and DBM with fibrous, fibrofatty and fatty tissues classified and displayed inside ROI

Obviously, the 5×25 -size patches are better classified than the others as seen in Figure 3. To show the effect of Equation (3), TPRs of each class are evaluated in each iteration, and Figure 4 shows the number of each class defined by Equation (3) and the TPRs corresponding to each iteration step for the patch size case of 5×25 and the 500-150 size of DBM. The trends of TPRs are asymptotically closed, which means that the classification is not significantly affected by the between-class imbalance degree.

Figure 5 shows the classification performance of one test vessel section by IB-IVUS method and DBM with 500-150 of hidden layers, and patch size of 5×25 . Figure 5(a) is a

B-mode image, Figure 5(b) shows the plaque area drawn by experts, and Figure 5(c) and Figure 5(d) show the classification performance of IB-IVUS and DBM, respectively. Obviously, in that IVUS image displays, IB-IVUS recognizes between fibrofatty and fibrous tissues not good as DBM does.

4. Conclusion. This study used deep Boltzmann machines to characterize IVUS signals. The bit level of data set was concerned. We presented an accumulative training selection method to train deep Boltzmann machines that was sensitive to misclassification rates. Although the research data set is relatively small, the experiments showed the accumulative effect of the proposed method.

This study proposed a training set selection as in Equation (3), and the parameter α was introduced to control the input number of each class. However, it was heuristically defined in the experiments. The optimal value of α should be studied as future work. In addition, the proposed method has been evaluated by comparison with the conventional method IB-IVUS. The evaluation of the proposed method needs more considerations in comparison with other methods in the literature of IVUS tissue characterization, or other traditional classifiers in the field of machine learning.

Acknowledgment. This study was supported by the Grant-in-Aid for Scientific Research, KAKENHI, of Japan Society for the Promotion of Science, Japan. The grant number is 16H02875.

REFERENCES

- [1] A. Katouzian, S. Sathyanarayana, B. Baseri, E. E. Konofagou and S. G. Carlier, Challenges in atherosclerotic plaque characterization with intravascular ultrasound (IVUS): From data collection to classification, *IEEE Trans. Inf. Technol. Biomed.*, vol.12, no.3, pp.315-327, 2008.
- [2] M. Kawasaki et al., Diagnostic accuracy of optical coherence tomography and integrated backscatter intravascular ultrasound images for tissue characterization of human coronary plaques, *J. Am. Coll. Cardiol.*, vol.48, no.1, pp.81-88, 2006.
- [3] A. Nair, B. D. Kuban, E. M. Tuzcu, P. Schoenhagen, S. E. Nissen and D. G. Vince, Coronary plaque classification with intravascular ultrasound radiofrequency data analysis, *Circulation*, vol.106, no.17, pp.2200-2206, 2002.
- [4] Y. LeCun, Y. Bengio and G. Hinton, Deep learning, *Nature*, vol.521, no.7553, pp.436-444, 2015.
- [5] G. E. Hinton, S. Osindero and Y. W. Teh, A fast learning algorithm for deep belief nets, *Neural Comput.*, vol.18, no.7, pp.1527-1554, 2006.
- [6] G. E. Hinton, A practical guide to training restricted Boltzmann machines, *Neural Networks: Tricks of the Trade*, pp.599-619, 2012.
- [7] F. Asja and I. Christian, Training restricted Boltzmann machines: An introduction, *Pattern Recognition*, vol.47, no.1, pp.25-39, 2014.
- [8] H. Larochelle, M. Mandel, R. Pascanu and Y. Bengio, Learning algorithms for the classification restricted Boltzmann machine, *J. Mach. Learn. Res.*, vol.13, pp.643-669, 2012.
- [9] N. T. Kuong, E. Uchino and N. Suetake, IVUS tissue characterization of coronary plaque by classification restricted Boltzmann machine, *JACIII*, vol.21, no.1, pp.67-73, 2017.
- [10] N. T. Kuong, E. Uchino and N. Suetake, IVUS tissue characterization in time-frequency domain using discriminative restricted Boltzmann machines, *Proc. of the 2017 RISP International Workshop on Nonlinear Circuits, Communications and Signal*, Guam, USA, pp.405-408, 2017.
- [11] N. T. Kuong, E. Uchino and N. Suetake, Coronary plaque classification with discriminative restricted Boltzmann machine and adaptive synthetic sampling, *Proc. of the 19th IEEE Hiroshima Section Student Symposium*, Shimane, Japan, pp.260-263, 2017.
- [12] G. S. Mintz et al., American college of cardiology clinical expert consensus document on standards for acquisition, measurement and reporting of intravascular ultrasound studies (IVUS), *J. Am. Coll. Cardiol.*, vol.37, no.5, pp.1478-1492, 2001.
- [13] R. Salakhutdinov and H. Larochelle, Efficient learning of deep Boltzmann machines, *Proc. of the 13th International Conference on Artificial Intelligence and Statistics*, Sardinia, Italy, pp.693-700, 2010.
- [14] Z. H. Zhou and X. Y. Liu, Training cost-sensitive neural networks with methods addressing the class imbalance problem, *IEEE Trans. Knowl. Data Eng.*, vol.18, no.1, pp.63-77, 2006.